

# DIRECT CONTACT HEAT TRANSFER WITH CHANGE OF PHASE: CO-CURRENT FLOW OF IMMISCIBLE FILMS WITH SURFACE EVAPORATION

ARYE GOLLAN and SAMUEL SIDEMAN

Department of Chemical Engineering, Technion—Israel Institute of Technology, Haifa, Israel

(Received 19 June 1967 and in revised form 15 March)

**Abstract**—Temperature profiles and heat transfer coefficients in two phase, liquid–liquid, stratified laminar flow down an inclined adiabatic plane were calculated numerically for the case where the thickness of the upper, volatile, liquid layer varies continuously due to surface evaporation. Approximate and asymptotic analytical solutions are presented for comparison.

With thin volatile films, heat-transfer coefficients of about 1000 cal/h °C m<sup>2</sup> can be realized, indicating the feasibility of utilising films, rather than, or in conjunction with, dispersions. The limitations imposed by the hydrostatic head on the latter can thus be overcome.

## NOMENCLATURE

|          |   |                  |   |
|----------|---|------------------|---|
| $a$ ,    | thickness of lighter film, $a(x)$ ;             | $T_w$ ,          | temperature at the solid plane;                         |
| $a_0$ ,  | thickness of lighter film, at $x = 0$ ;         | $V_i$ ,          | velocity of phase $i$ ;                                 |
| $c_n$ ,  | coefficients, equation (15);                    | $\bar{V}$ ,      | velocity, average;                                      |
| $C_p$ ,  | specific heat capacity;                         | $V_f$ ,          | velocity of free interface, heavy fluid;                |
| $E$ ,    | dimensionless group, equation (20);             | $V_{2f}$ ,       | velocity of liquid–liquid interface;                    |
| $g$ ,    | gravitational acceleration;                     | $V_s$ ,          | velocity of free interface, light fluid;                |
| $G_z$ ,  | Graetz number, modified ( $\equiv Pe_f/\xi$ );  | $x$ ,            | cartesian coordinate;                                   |
| $H$ ,    | total thickness of films ( $h_0 + a$ );         | $y$ ,            | cartesian coordinate;                                   |
| $h_x$ ,  | heat-transfer coefficient, local;               | $z$ ,            | cartesian coordinate ( $\equiv -y$ ).                   |
| $h_L$ ,  | heat-transfer coefficient, average;             | Greek symbols    |   |
| $h_0$ ,  | thickness of heavy film;                        |                  |   |
| $k_i$ ,  | thermal conductivity;                           | $\alpha_i$ ,     | thermal diffusivities, $(k/\rho C_p)$ ;                 |
| $K$ ,    | ratio of interfacial velocities, equation (21); | $\beta$ ,        | inclination angle of flow to horizontal;                |
| $L$ ,    | length of flow section ( $x = L$ );             | $\gamma$ ,       | ratio of densities, $(\rho_1/\rho_2)$ ;                 |
| $Pe_f$ , | Péclet number ( $\equiv V_f h_0/\alpha_2$ );    | $\eta$ ,         | dimensionless coordinate ( $y/h_0$ );                   |
| $q_x$ ,  | heat flux, at $x = x$ ;                         | $\theta$ ,       | temperature, dimensionless $[T - T_s]/(T_0 - T_s)$ ;    |
| $R$ ,    | dimensionless group $(k_1 h_0/k_2 a_0)$ ;       | $\bar{\theta}$ , | temperature, dimensionless $(1 - \theta)$ ;             |
| $Re$ ,   | Reynolds number;                                | $\theta_f$ ,     | temperature, dimensionless, at liquid–liquid interface; |
| $Re_w$ , | water film $Re$ number;                         | $\lambda$ ,      | latent heat of evaporation;                             |
| $T$ ,    | temperature, $T(x, y)$ ;                        | $\lambda_m$ ,    | eigenvalues;  |
| $T_f$ ,  | temperature, liquid–liquid interface, $T(x)$ ;  | $\nu_i$ ,        | kinematic viscosities;                                  |
| $T_0$ ,  | inlet temperature of phase 2;                   | $\rho_i$ ,       | densities;  |
| $T_s$ ,  | temperature of free interface;                  | $\tau$ ,         | ratio of kinematic viscosities $(\nu_1/\nu_2)$ ;        |
|          |   | $\xi$ ,          | dimensionless axial coordinate $(x/h_0)$ ;              |

- $\zeta$ , dimensionless coordinate ( $z/h_0$ );  
 $\omega$ , dimensionless height ( $H/h_0$ ).

#### Subscripts

- 1, upper phase;  
 2, lower phase;  
 $f$ , liquid-liquid interface;  
 $i$ , phase number (1—lighter fluid; 2—heavier fluid);  
 $i, x$ , phase  $i$ , axial position  $x$ , ( $x = 0$ ,  $x = x$  or  $x = L$ );  
 $L$ , average, up to  $x = L$ ;  
 0, initial, at  $x = 0$ ;  
 $s$ , free interface;  
 $w$ , wall;  
 $x$ , local, at  $x = x$ .

#### INTRODUCTION

THE ELIMINATION of solid transfer surfaces by utilizing an evaporating immiscible liquid in direct contact heat-transfer affects low scale formation and efficient heat transfer at low temperature driving forces. Multi-phase, direct contact, heat exchangers have thus gained importance in water desalination schemes, where heat recovery at low temperature driving forces is of paramount economic value.

Detailed studies of single and multi-particle systems undergoing change of phase [1-3] showed that the hydrostatic head in such dispersed systems imposes a severe limitation on the transfer efficiency. A water head of one and a half foot can increase the boiling point by, roughly, 1 degC. Thus the effective driving force decreases with an increase in the hydrostatic head, and, at low nominal driving forces and high depths, negative driving forces may prevail. By utilizing phase change in films, rather than or in conjunction with dispersions, a more efficient multi phase exchanger is anticipated.

A recent theoretical and experimental study [4] of discrete films of a volatile fluid undergoing change of phase while floating on a stagnant, infinitely large expanse of water, provided the lower bound values of the heat-

transfer coefficients to be expected when utilizing films in multiphase exchangers.

This paper presents a theoretical study of the temperature distribution and heat-transfer coefficients to be expected when a thin film of volatile fluid, say pentane, is evaporating, hence diminishing, while flowing co-currently and in direct contact with a laminar water film down a slightly inclined adiabatic plane. It is noteworthy that although theoretical analysis [5, 6] predicts unstable film flow at any Reynolds number, laminar, ripple-free films were observed by these authors on a near horizontal plane. Similar observations were also reported by Goodridge and Gartside [7] for Reynolds numbers up to 1000. Also, stable ripple free flow was maintained when a thin pentane layer was added on top of the water layer under similar flow conditions [10].

A piece-wise Graetz type solution, accounting for the variable evaporating film thickness, can be obtained [9] based on a recent Graetz-type solution presented by Bentwich and Sideman [8]. However, the solution for the eigenfunctions and corresponding eigenvalues requires tedious computations, and the ensuing results are restricted to the initially stipulated physical properties and film thickness. Hence, a numerical solution of the differential equations is actually more general in the practical sense, since all physical properties and initial dimensions constitute input data and are independent of the solution procedure. Since the exact solution may require considerable computer time it was deemed advantageous to study the effect of simplifying assumptions. Thus, in addition to the exact "double grid" solution, two approximate numerical solutions as well as two (essentially asymptotic), analytical solutions are presented here in brevity. The various models treated are summarized in Fig. 1.

#### MATHEMATICAL MODELS

##### 1. The exact "double grid" model

We consider the case of two-dimensional, stratified, two-phase laminar flow down a solid

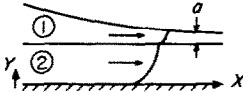
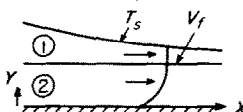
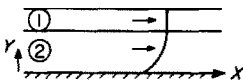
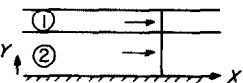
|   |  |  |
|---|--|--|
| 1. EXACT, DOUBLE GRID MODEL :   |  |  |
|  | $V_1 = V_1(x, y)$<br>$V_2 = V_2(x, y)$                     | $a = a(x)$<br>$T_1 = T_1(x, y)$<br>$T_2 = T_2(x, y)$   |
| 2. "LINEAR" MODEL :   |  |  |
|  | $V_1 = V_f = \text{Const.}$<br>$V_2 = V_2(y)$              | $a = a(x)$<br>$T_1 = T_s + A(x)Y$<br>$T_2 = T_2(x, y)$ |
| 3. CONSTANT THICKNESS MODEL :   |  |  |
|  | $V_1 = V_f = \text{Const.}$<br>$V_2 = V_2(y)$              | $a = a_0$<br>$T_1 = T_s + A(x)Y$<br>$T_2 = T_2(x, y)$  |
| 4. CONSTANT THICKNESS & VELOCITY MODEL (analytical) :                             |  |  |
|  | $V_1 = V_f = \text{Const.}$<br>$V_2 = V_f = \text{Const.}$ | $a = a_0$<br>$T_1 = T_s + A(x)Y$<br>$T_2 = T_2(x, y)$  |
| 5. DITTO, SHORT CONTACT TIME (analytical)   |  |  |
|   | ditto ;  | ditto ; ditto ;  |

FIG. 1. Summary of mathematical models.

plane inclined at an angle  $\beta$ . The two liquids are immiscible and differ in their physical properties. It is assumed that the flow is viscous, fully developed, laminar as well as stable, and hence governed by the Navier-Stokes' equations in which time partial derivatives are zero. The solid plane is adiabatic, and the temperature at the solid plane,  $T_w$ , varies with length  $x$ . The atmosphere is at a constant uniform temperature,  $T_s$ , representing the boiling point of the light fluid at the corresponding pressure of the system. With cartesian coordinates  $x - y$  as shown in Fig. 2, the temperature distribution  $T(x, y)$  throughout the space  $x \geq 0, 0 \leq y \leq H$  is evaluated for an arbitrary temperature distribution  $T(0, y)$  at the cross section  $x = 0$ . The amount of heat conducted downstream is considered negligible, compared with that transferred by convection in this direction.

By the momentum equation the  $x$ -directed velocities of the two fluids are:

$$V_1 = \frac{g \cdot h_0^2}{v_1} \sin \beta \left\{ \frac{1}{2}(\omega - 1)^2 + \tau[(\omega - 1)\gamma + \frac{1}{2}] - \frac{1}{2}(\omega - \eta)^2 \right\}; \quad 1 \leq \eta \leq \omega$$

$$V_2 = \frac{g \cdot h_0^2}{v_2} \sin \beta \{ [\omega\gamma - (\gamma - 1)]\eta - \frac{1}{2}\eta^2 \}; \quad 0 \leq \eta \leq 1$$
(1)

where, in reference to Fig. 2,

$$H \equiv h_0 + a; \quad \omega \equiv H/h_0;$$

$$\eta \equiv Y/h_0; \quad \gamma \equiv \rho_1/\rho_2; \quad \tau \equiv v_1/v_2.$$

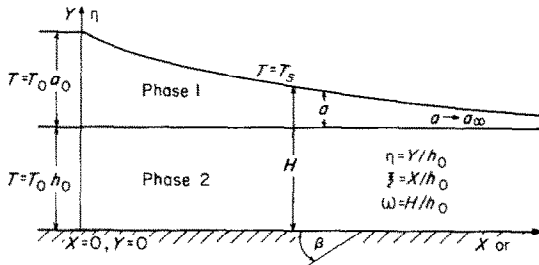


FIG. 2. Schematic presentation of coordinates.

The dimensionless equations governing the heat transfer in the two phases are

$$\frac{\partial^2 \theta}{\partial \eta^2} = \left[ \frac{V_i h_0}{\alpha_i} \right] \frac{\partial \theta}{\partial \xi}; \quad i = 1; \quad 1 \leq \eta \leq \omega \quad (2)$$

$$\frac{\partial^2 \theta}{\partial \eta^2} = \left[ \frac{V_i h_0}{\alpha_i} \right] \frac{\partial \theta}{\partial \xi}; \quad i = 2; \quad 0 \leq \eta \leq 1$$

subject to the boundary conditions

$$\frac{\partial \theta}{\partial \eta_-} = \frac{k_1}{k_2} \frac{\partial \theta}{\partial \eta_+} \quad \xi \geq 0; \quad \eta = 1 \quad (3)$$

$$\frac{\partial \theta}{\partial \eta} = 0 \quad \xi \geq 0; \quad \eta = 0 \quad (4)$$

$$\theta = 0 \quad \xi \geq 0; \quad \eta = \omega \quad (5)$$

$$\theta = 1 \quad \xi = 0; \quad 0 \leq \eta \leq \omega \quad (6)$$

$$\frac{da}{d\xi} = \frac{(T_0 - T_s) k_1}{\lambda_1 V_s \rho_1} \frac{\partial \theta}{\partial \eta} \quad \xi = 0; \quad \eta = \omega \quad (7)$$

where;

$$\theta = \frac{T - T_s}{T_0 - T_s}; \quad \xi = \frac{x}{h_0}.$$

Equation (7) relates the local mass of the volatile fluid evaporating at the upper free surface (the heat sink) with the temperature and the gas-liquid interfacial velocity  $V_s$ . The term which accounts for the sensible heat change of the evaporating mass is negligible.

The local heat flux is calculated by:

$$q_x = - \frac{k_2}{h_0} \frac{\partial \theta}{\partial \eta} \bigg|_{\eta=1} (T_0 - T_s) \quad (8)$$

and the corresponding local and average heat-transfer coefficient defined in terms of the

average, mixing-cup temperatures  $\theta_{1,x}$  and  $\theta_{2,x}$  are given by:

$$h_x \equiv \frac{k_2}{h_0 [\theta_{2,x} - \theta_{1,x}]} \frac{\partial \theta}{\partial \eta} \bigg|_{\eta=1} \quad (9)$$

$$h_L \equiv \frac{1}{L} \int_0^L h_x dx \quad (11)$$

where

$$\bar{\theta}_{1,x} = \frac{1}{(\omega - 1) \cdot \bar{V}_1} \int_1^\omega \theta V_1 d\eta;$$

$$\bar{\theta}_{2,x} = \frac{1}{\bar{V}_2} \int_0^1 \theta V_2 d\eta. \quad (10)$$

The double suffix denotes the phase and the axial distance, respectively. The corresponding finite difference equations are quite simple and are not given here.

## 2. A linear model

For very thin volatile films, i.e.  $a/h_0 \ll 1$  (say 1/40),  $\omega \rightarrow 1$  and equation (1) reduces to:

$$\left. \begin{aligned} V_1 &\simeq \frac{gh_0^2}{2v_2} \sin \beta = V_f; & 1 \leq \eta \leq \omega \\ V_2 &\simeq \frac{gh_0^2}{v^2} \sin \beta \left[ \eta - \frac{\eta^2}{2} \right]; & 0 \leq \eta < 1. \end{aligned} \right\} \quad (1a)$$

Equation (2) and boundary conditions (3–5) remain unchanged. As will be shown in the discussion, a linear temperature distribution is established in the thin volatile film practically at the inlet. Thus, the initial condition, equation (6) is taken as

$$\theta = 1 + \frac{h_0}{a_0} (1 - \eta); \quad \xi = 0; \quad 1 \leq \eta \leq \omega \quad (6a)$$

$$\theta = 1; \quad \xi = 0; \quad 0 \leq \eta \leq 1 \quad (6b)$$

and equation (7) now becomes

$$\frac{h_0}{a} \frac{k_1}{V_f \rho_1} \theta_f - \frac{a}{2} C_{p1} \frac{d\theta_f}{d\xi} = \frac{\lambda_1}{(T_s - T_0)} \frac{da}{d\xi} \quad (7a)$$

where the term accounting for the change of

the sensible heat of the evaporating mass was neglected.

In accordance with the initial boundary condition, equation (6a), the solution for the thin upper film is assumed to be linear throughout; i.e.

$$\theta = \theta_f \left[ 1 + \frac{h_0}{a} (1 - \eta) \right] \quad (12)$$

where  $\theta_f$ , the interfacial (liquid-liquid) temperature, as well as  $a$  are function of  $\xi$ . Note that at  $\xi = 0$ ,  $\theta_f = 1$ .

The temperature linearity assumed in the upper phase reduces the problem to the simultaneous solution of equation (2) with boundary conditions (3, 4, 6b, 7a), in the  $0 \leq \eta \leq 1$  region equations (8-11) obviously remain unchanged. Note, however, that equations (10) and (12) yield  $\bar{\theta}_{1,x} = \bar{\theta}_f/2$  and that equation (9) can also take the following form:

$$h_x \equiv \frac{k_1}{a} \frac{\theta_f}{\bar{\theta}_{2,x} - \bar{\theta}_{1,x}}. \quad (9a)$$

#### (a) A constant thickness model

For somewhat thicker films, say  $a/h_0 \simeq \frac{1}{10}$ , film thickness does not vary appreciably, and the solution is further simplified by assuming  $a = a_0$ . Though now much less justified on physical grounds, equations (1a) and (12) are assumed to hold. The problem is now completely described by equations (2) (for  $0 \leq \eta \leq 1$ ) (3, 4, 6a, 6b), but with  $a = a_0 = \text{constant}$ . Once the temperature profiles in the lower phase are determined, the heat-transfer coefficients can be determined as in the previous model.

#### 4. Asymptotic solution for small Graetz numbers

As in cases (2) and (3), the temperature in the thin volatile film is assumed to be linear, equation (12). Moreover,  $a$  is assumed constant ( $= a_0$ ) and the velocities of both phases are assumed constant and equal to  $V_f$ . The temperature distribution in the lower, heavier, film is

now obtained by solving the following dimensionless equation:

$$\frac{\partial^2 \theta}{\partial \eta^2} = Pe_f \frac{\partial \theta}{\partial \xi}; \quad Pe_f \equiv \frac{V_f h_0}{\alpha_2} \quad (13)$$

together with the boundary conditions given by equations (3, 4, 6b). Note that  $V_f = \frac{3}{2} V_2$ . The solution is given by:

$$\theta = \sum_{n=1}^{\infty} C_n \cos(\lambda_n \eta) \exp[-\lambda_n^2/G_z] \quad (14)$$

where,

$$G_z = Pe_f/\xi; \quad C_n = \frac{2 \sin \lambda_n}{\lambda_n + \frac{1}{2} \sin 2\lambda_n} \quad (15)$$

and the eigenvalues are calculated from

$$\lambda_n \tan \lambda_n = \frac{h_0 k_1}{a_0 k_2}. \quad (16)$$

The local heat-transfer coefficient, as defined by equation (9), is given by:

$$h_x = \frac{k_2}{h_0} \frac{\sum_{n=1}^{\infty} C_n \lambda_n \sin \lambda_n \exp[-\lambda_n^2/G_z]}{\sum_{n=1}^{\infty} C_n \left( \frac{\sin \lambda_n}{\lambda_n} - \frac{1}{2} \cos \lambda_n \right) \exp[-\lambda_n^2/G_z]} \quad (17)$$

A rather good approximation for large values of  $\xi$  (or small values of Péclet numbers) is obtained by utilizing the first term of the series solution only. Equation (17) then reduces to:

$$h_x = h_L \simeq \frac{k_2}{h_0} \left[ \frac{2\lambda_1^2}{2 - \lambda_1 \cot \lambda_1} \right] = \frac{k_1}{a_0} \left[ \frac{2\lambda_1}{2 \tan \lambda_1 - \lambda_1} \right]. \quad (18)$$

Since  $h_x$  is now  $x$ -independent it is also equal to  $h_L$ .

The utilization of equation (18) as an asymptotic solution for the variable-thickness film case is discussed below.

#### 5. Asymptotic solution for large Graetz numbers

In addition to the assumptions made in

case (4), (i.e.  $a = a_0$ ,  $V_1 = V_2 = V_f$  and a linear temperature distribution in the volatile film), it is further assumed that the heat penetration depth in the heavier phase, perpendicular to the interface, is very small in relation to its absolute thickness,  $h_0$ . Obviously this assumption implies that the temperature beyond the penetration depth remains unchanged, at  $T_0$ , and is justified only for short distances or short contact times.

Defining, for convenience, new dimensionless parameter

$$\bar{\theta} \equiv 1 - \theta = \frac{T - T_0}{T_s - T_0};$$

$$\bar{\theta}_f \equiv 1 - \theta_f = \frac{T_f - T_0}{T_s - T_0}; \quad \zeta = -\eta = \frac{z}{h_0};$$

where  $z = (-y)$  is a newly defined co-ordinate starting at, and perpendicular to, the interface ( $z = 0$  at  $y = h_0$ ). Clearly, the penetration concept implies that formally  $h_0 \rightarrow \infty$  (in the new  $z$ -coordinates).

The governing equation and boundary conditions are given by equations (13, 3, 6b), rewritten in the new dimensionless parameters, and equation (4) which now becomes

$$\bar{\theta} = 0; \quad \zeta = \infty; \quad \xi \geq 0 \quad (4a)$$

yielding

$$\bar{\theta} = -\exp[R\zeta] \exp[R^2/G_z] \operatorname{erfc}[R/G_z^{\frac{1}{2}} + \frac{1}{2}\zeta G_z^{\frac{1}{2}}] \quad (19)$$

and

$$\bar{\theta}_f = 1 - \exp[R^2/G_z] \operatorname{erfc}[R^2/G_z]^{\frac{1}{2}} \equiv 1 - E \quad (20)$$

where,

$$R \equiv \frac{h_0 k_1}{a_0 k_2}.$$

The local heat-transfer coefficient defined by equations (9) and (9a) are given by:

$$h_x = \frac{2k_1}{a} \frac{1 - \bar{\theta}_f}{\bar{\theta}_f + 1} = \frac{2k_1}{a} \frac{E}{2 - E} \quad (9b)$$

and the average heat-transfer coefficient, as

defined by equation (11), is conveniently obtained either by numerical or graphical methods.

## RESULTS AND DISCUSSION

The numerical solution to cases 1 to 3 were obtained by an Elliott 503 computer utilizing the straightforward explicit finite difference method.

Comparison of the various cases treated is best demonstrated in Fig. 3 where the calculated interfacial temperatures are plotted as a function of the axial distance.

As is to be expected the linear approximation (case 2) is very good for very thin films but yields erroneous results for thicker films, particularly near the inlet. As will be shown below, the discrepancy is due to the non-linearity of the temperature profile near the inlet as well as the existence of a velocity distribution in the thick volatile film.

The constant thickness models (cases 3 and 4) are seen to represent good approximations for

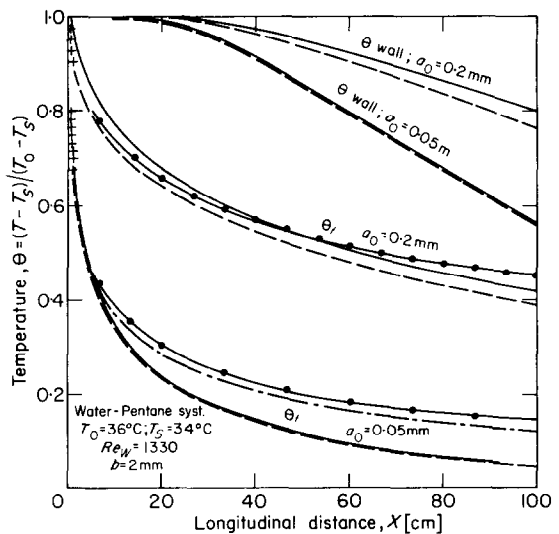


FIG. 3. Development of interfacial and wall temperatures along the plate.

- Double grid (case 1).
- - - Linear (case 2).
- · - Constant thickness (case 3).
- · · Constant  $a_0$  and  $V$ , analytical (case 4).
- + + + Short contact time (case 5).

thick films, though the assumption of a linear temperature profile increases their inaccuracy near the inlet. As is also evident from Fig. 3, the application of these two models (3 and 4) to thin films will obviously yield erroneous results.

Lastly, the solution for "short contact times" (case 5) is obviously limited for the entry region only, or else for systems with large Péclet numbers, i.e. small thermal diffusivities. This solution is best suited to very thin films, where the constant velocity and the linearity assumptions, inherent in the derivation, hold. The error introduced by assuming  $V_1 = V_f$  in all, but the exact, models can be determined as a function of the relative thicknesses of the two films. Defining  $K = V_f/V_{2f}$  where  $V_f = V_1$  [by equation (1a)] and  $V_{2f}$  is the velocity of the liquid-liquid interface [by equation (1)], it can easily be shown that

$$\frac{a_0}{h_0} = \frac{1}{2\gamma} \frac{1-K}{K}. \quad (21)$$

For the system considered here ( $h_0 = 0.2$  cm,  $\gamma = 0.63$ ) the assumption that  $V_1 = V_f$  introduces an error of 3 per cent for  $a = 0.005$  cm, whereas for  $a_0 = 0.02$  cm the error is almost 10 per cent. Thus, as clearly indicated by Fig. 3, the error for  $h_0/a_0 \geq 40$  is better than 3 per cent.

The temperature linearity assumed in all, but the exact, models can be checked by plotting the calculated temperature profiles in the volatile film for various values of  $a_0$  and comparing these profiles to equation (12). Figure 4 represents such a comparison for  $a_0 = 0.02$  cm. The agreement with thin films is very good practically from the start, making the graphical presentation superfluous. The temperature profiles in the water phase are shown in Fig. 5, along with average temperatures at various longitudinal cross sections.

The accumulated change of the volatile film thickness is shown in Fig. 6 for two initial film thicknesses, calculated by the exact and the linear models. The results, practically identical

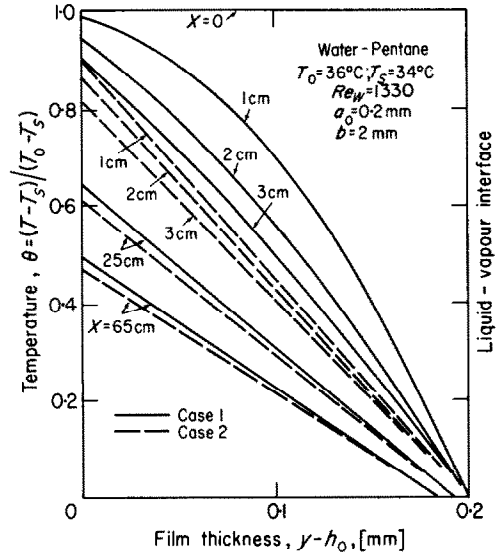


FIG. 4. Temperature profiles in the pentane film.

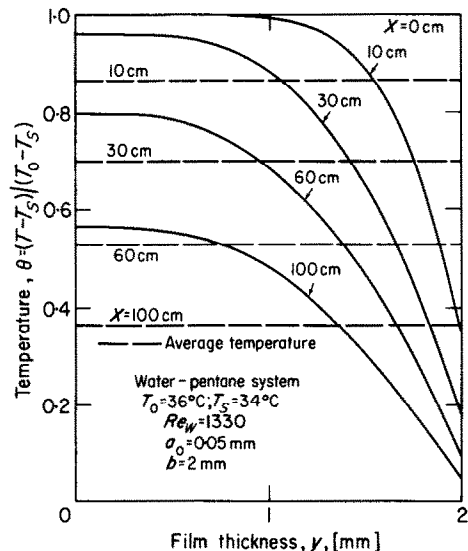


FIG. 5. Temperature profiles in the water film (case 1).

in the graphical presentation, substantiate the above conclusions regarding the applicability of the linear model.

Equation (18), (case 4) represents the asymptotic solution for the variable thickness case for small  $G_z$  Numbers, (or large values of  $\zeta$ ). Obviously, this solution is applicable only if

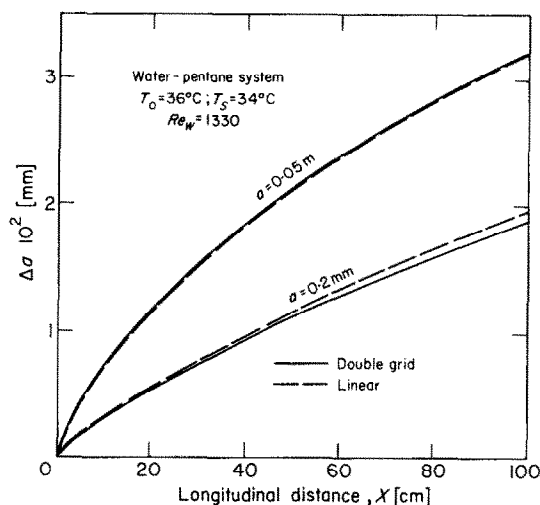


FIG. 6. Variation of film-thickness with plate length.

the volatile film exists and is yet unbroken. Under these conditions the temperature of both phases asymptotically approach the value of  $T_s$  and the asymptotic value of  $a$ , i.e.  $a = \text{const}$ , should replace the value of  $a_0$  in equations (16) and (18). This value can be obtained by a simple heat and mass balance since now

$$\int_0^{h_0} VT \, dy \simeq \bar{V} T_s$$

where  $\bar{V}$  denotes the average velocity.

The exact local and average fluxes and their respective local and average heat-transfer coefficients are shown in Fig. 7. Figure 8 represents a comparison of the average heat-transfer coefficients calculated by the exact and linear models. Also included in Fig. 8 are the asymptotic solutions for large and small  $G_z$  numbers. The results are clearly in accord with the conclusions drawn above from Fig. 3.

### CONCLUSIONS

An exact solution for heat transfer in two phase flow with variable film thickness was obtained and the effect of simplifying assumptions was studied. The linear temperature assumption in the variable thickness model

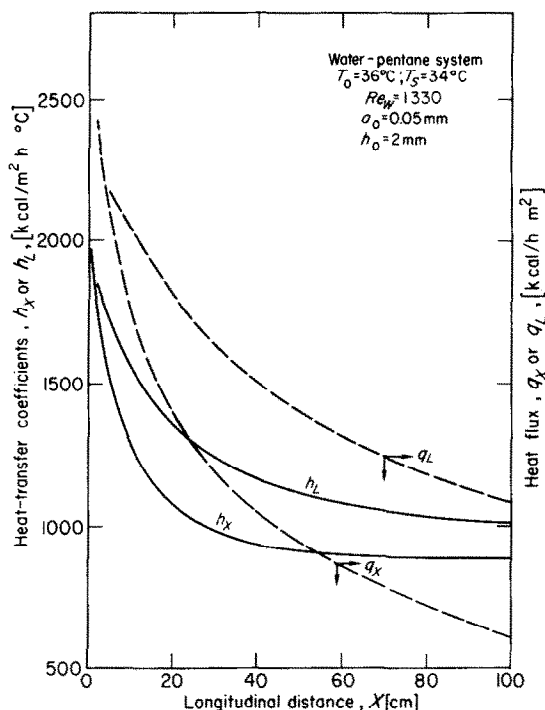


FIG. 7. Average and local fluxes and heat-transfer coefficients (case 1).

is, within an error of 10 per cent, suitable even for relatively thick,  $h_0/a_0 \simeq 10$ , films. This assumption is better than 3 per cent for thin,  $h_0/a_0 \geq 40$ , films. The constant thickness models are particularly useful for thick layers, and, due to compensation of the assumption made, are fast and surprisingly accurate.

The high transfer coefficients calculated here for laminar, stable flow, possible at small inclination angles, introduce an interesting practical problem. Presumably, turbulent flow should yield even higher transfer coefficients. However turbulence will undoubtedly break the upper thin film, and reduce the actual contact area. Thicker, "unbreakable" films will obviously introduce higher resistance to heat transfer and are undesirable under any conditions. Thus, the practical question presently posed is whether turbulent flow with partial coverage is more efficient than laminar flow with



total coverage. Work in this direction is presently underway.

Thanks are due to Professor M. Bentwich of the Department of Mechanical Engineering for his continued interest in the subject.

## REFERENCES

1. S. SIDEMAN and Y. TAITEL, Direct contact heat transfer with change of phase: evaporation of drops in an immiscible liquid medium, *Int. J. Heat Mass Transfer* 7, 1273 (1964).
2. S. SIDEMAN and G. HIRSCH, Direct contact heat transfer with change of phase: condensation of single vapor bubbles in an immiscible liquid medium—preliminary studies, *A.I.Ch.E. J.* 11, 1019 (1965).
3. S. SIDEMAN and Y. GAT, Direct contact heat transfer with change of phase: spray-column studies of a three-phase heat exchanger, *A.I.Ch.E. J.* 12(2), 296 (1966).
4. M. BENTWICH, U. LANDAU and S. SIDEMAN, Direct contact heat transfer with change of phase: evaporation of discrete volatile films from the surface of a stagnant immiscible liquid, Technion Research and Development Foundation Proj. CE-37, Report No. 16, to the Israel National Council for Research and Development (January 1967).
5. T. B. BENJAMINE, Wave formation in laminar flow down an inclined plane, *J. Fluid Mech.* 2, 554 (1957).
6. C. S. YIH, Stability of liquid flow down an inclined plane, *Physics Fluids* 6(3), 321 (1963).
7. F. GOODRIDGE and G. GARTSIDE, Mass transfer into near-horizontal liquid films. Part 1: Hydrodynamic Studies, *Trans. Instn Chem. Engrs.* 43, T. 62 (1965).
8. M. BENTWICH and S. SIDEMAN, Temperature distribution in cocurrent two-phase (liquid-liquid) laminar flow on inclined surfaces, *J. Heat Transfer* 86(4), 476 (1964).
9. S. SIDEMAN and A. GOLLAN, Direct heat transfer with change of phase between immiscible films in co-current flow (in Hebrew), Technion Research and Development Foundation Project CE-37A Report No. 17 to the Israel National Council for Research and Development (January 1967).
10. A. GOLLAN and S. SIDEMAN, Direct contact heat transfer with change of phase: co-current flow of immiscible film with surface evaporation. Technion Research and Development Foundation Project CE-37A, Report No. 18 to the Israeli National Council for Research and Development (September 1967).

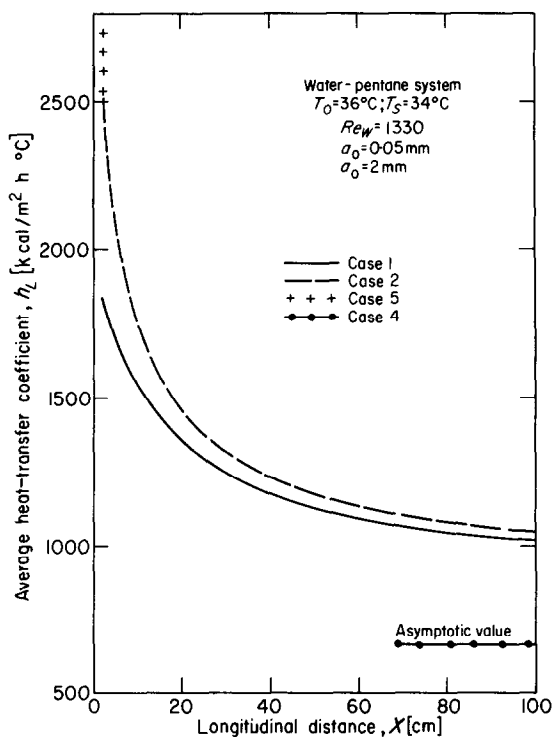


FIG. 8. Average heat-transfer coefficients.

## ACKNOWLEDGEMENT

The authors wish to thank the Israeli National Council for Research and Development for their continued support of this work.

**Résumé**—Les profils de température et les coefficients de transport de chaleur dans un écoulement laminaire stratifié à deux phases liquides le long d'un plan incliné adiabatique ont été calculés numériquement dans le cas où la couche supérieure est un liquide volatil dont l'épaisseur varie d'une façon continue à cause de l'évaporation de la surface. On présente dans un but de comparaison des solutions analytiques approchées et asymptotiques.

On peut réaliser, avec des films volatils de faible épaisseur, des coefficients de transport de chaleur d'environ  $1,1 \text{ KW}/^\circ\text{cm}^2$ , ce qui indique la possibilité d'utiliser des films, plutôt que, ou en même temps que des dispersions. Les limitations imposées par la pression hydrostatique sur ces dernières peuvent ainsi être surmontées.

**Zusammenfassung**—Temperaturprofil und Wärmeübergangskoeffizienten für zwei Phasen, Flüssigkeit-Flüssigkeit-Schichtströmung an einer geneigten adiabaten Ebene wurden numerisch berechnet für den Fall, dass sich die Verdunstung stetig ändert. Angenäherte und asymptotische analytische Lösungen werden

vergleichsweise angegeben. Mit dünnen flüchtigen Filmen lassen sich Wärmeübergangskoeffizienten von etwa  $1,2 \text{ W/m}^2 \text{ grad}$  erhalten was die Möglichkeit bietet, Filme allein oder in Verbindung mit Dispersionen zu verwenden. Die von der hydraulischen Höhe ausgehende Begrenzung bei letzteren fällt damit weg.

**Аннотация**—Численно рассчитаны температурные профили и коэффициенты теплообмена для слоистого ламинарного течения одной жидкости по другой вниз по наклонной адиабатической плоскости. Принимается, что толщина верхнего слоя летучей жидкости непрерывно изменялась за счёт испарения с открытой поверхности. Проводятся сопоставления численных результатов с приближенными и асимптотическими аналитическими решениями. Показано, что в случае тонких пленок летучих жидкостей реализуемы коэффициенты теплообмена порядка  $1000 \text{ кал/час С м}^2$ .